

A comparative study of deep neural network architectures with chaotic optimization for electroencephalography-based emotion recognition

Zahraa Tarek¹, Khaled Alnowaiser², and Esraa Hassan^{3*}

¹ Department of Computer Engineering and Information, College of Engineering, Wadi Ad Dwaser, Prince Sattam Bin Abdulaziz University, Al-Kharj, Saudi Arabia

² Department of Computer Science, College of Computer Engineering and Sciences, Prince Sattam Bin Abdulaziz University, Al-Kharj, Riyadh, Saudi Arabia

³ Department of Machine Learning and Information Retrieval, Faculty of Artificial Intelligence, Kafrelsheikh University, Kafr El Sheikh, Kafr El Sheikh, Egypt

z.elmana@psau.edu.sa; k.alnowaiser@psau.edu.sa; esraa.hassan@ai.kfs.edu.eg

ARTICLE INFO

Article history:

Received: March 10, 2026

Revised: April 20, 2026

Accepted: April 23, 2026

Published Online: May 21, 2026

Keywords:

Deep neural architectures

Chaotic optimization

Electroencephalography-based emotion recognition

ABSTRACT

Electroencephalography (EEG)-based emotion recognition has become an important research direction in affective computing, driven by its applications in mental health assessment, human-computer interaction, and brain-machine interfaces. Despite recent progress, challenges persist due to the high dimensionality of EEG features and the absence of consensus on optimal deep learning architectures for reliable emotion classification. This study introduces a unified comparative framework for EEG emotion recognition that combines statistical feature extraction with chaos-enhanced deep learning optimization. Five representative neural architectures, Transformer-based, CNN-LSTM hybrid, residual multilayer perceptron (MLP), capsule network, and hyperbolic-inspired network, were systematically evaluated under identical experimental conditions. EEG signals were normalized and transformed using advanced statistical feature extraction techniques, followed by robust data augmentation to improve model generalization. A chaos-driven learning rate optimization strategy based on the logistic map was incorporated into the training process to promote stable convergence and reduce susceptibility to local minima. Experimental results demonstrated that chaotic optimization substantially improved training stability and overall classification performance across architectures. The hyperbolic-inspired network achieved the highest validation accuracy of 93.21% with a validation loss of 0.197 and a training time of 19.09 s, followed closely by the residual MLP, which attained 91.80% accuracy with a loss of 0.226. The capsule network also showed competitive performance (90.87% accuracy), whereas the CNN-LSTM hybrid exhibited comparatively lower accuracy (70.73%). These findings underscore the effectiveness of chaos-driven optimization and provide practical insights into architecture selection for efficient and robust EEG-based emotion recognition. The proposed framework offers a reproducible benchmark to support informed model design in affective computing applications.



1. Introduction

Electroencephalography (EEG) signals for emotion recognition have been of interest in the last

few years. This is because emotion recognition assists in computing, mental health surveillance, neurofeedback systems, and adaptive human-computer interactions. EEG does not rely on fa-

* Corresponding Author

cial expressions and behavior.^{1–3} Emotion recognition based on EEG is not yet perfected due to the non-linearity of the signal and the high dimensionality of the data and the subject. Standard approaches to machine learning of EEG emotion classification typically include handcrafted features and shallow classifiers.^{4–6} The common machine learning approach to EEG emotion classification does not always yield nonlinear correlations in brain signals.

Deep learning enables feature learning and hierarchical representation extraction. Convolutional neural networks (CNNs), recurrent neural networks, and Transformer-based models work well on EEG-related tasks. The performance of the models depends a lot on design choices, optimization methods, and training stability.^{7–9} A major challenge in EEG-based learning is optimization. Standard gradient-based optimizers can converge to suboptimal solutions, particularly when the data is noisy and the feature space is high-dimensional. Chaos-inspired optimization techniques have gained popularity because they enhance exploration of the search space, accelerate convergence, and help avoid local minima.^{10–13} Chaotic maps, such as the one shown, add controlled randomness to chaos-inspired optimization techniques and provide a clear way to adjust the learning rate over time. Because of these challenges, this work builds an experimental framework that tests several deep learning architectures for EEG-based emotion recognition using a chaos-driven optimization scheme. Specifically, five distinct neural models, Transformer-based, CNN–long short-term memory (LSTM) hybrid, residual multilayer perceptron (MLP), capsule networks, and hyperbolic-inspired networks, were implemented and trained using identical data preprocessing, augmentation, and evaluation protocols.^{14–16} A logistic map-based chaotic learning rate modulation was integrated into the training process to improve robustness and convergence stability. The primary contributions of this study are threefold:

- (i) A comprehensive comparison of diverse deep learning architectures for EEG emotion recognition using statistical EEG features;
- (ii) The integration of chaotic optimization into model training to enhance learning dynamics and generalization; and
- (iii) A reproducible benchmarking framework that facilitates fair evaluation and informed architecture selection.

The experimental results provide valuable insights into the trade-offs between model complexity, performance, and optimization behavior, advancing the development of reliable EEG-based emotion recognition systems.

2. Related works

Recent advances in affective computing have highlighted the growing importance of EEG-based emotion recognition, given its direct link to neural activity and broad applicability across brain–computer interfaces, neurofeedback systems, mental health monitoring, and human–computer interaction, as illustrated in **Table 1**. The following works represent key contributions that collectively illustrate the evolution of EEG-based emotion recognition, ranging from hybrid reservoir and transformer models to biologically inspired data augmentation techniques and large-scale systematic reviews of current methodologies.

Guo et al.⁸ proposed the ESN–TLC model, a combination of an echo state network (ESN), a Transformer block, an LSTM, and a CNN, achieving an accuracy of 93%. On the DEAP dataset, arousal accuracy was 93.9%, and valence accuracy was 94.2%. The model studies how reservoir duration affects deep-reading classifiers, assists in determining the maximum acceptable parameter preference, and demonstrates that ESN outperforms conventional methods in terms of accuracy and computational efficiency. This combination enhances the temporal dynamics and spatial capabilities of EEG records, which are essential for applications such as the popularization of individual emotions, adaptive neurofeedback, and brain region analysis (BRA). Zheng et al.¹⁵ proposed a new data augmentation model, the gustatory-emotion coupling model with multiblock attention module (GECM-MBAM), to complement emotion recognition. The model replicated the 1/f characteristics and synchronization in brain responses observed via EEG, and validated bionic processing for EEG signal security. MBAM, mainly based on GECM features, facilitates emotion-related EEG statistics enhancement. Experiments indicate that GECM-MBAM significantly outperformed current data augmentation models in reputation accuracy and achieved higher overall performance metrics (96.91% accuracy on the SEED dataset, 94.52% on the SEED-IV dataset) than state-of-the-art algorithms. This model provides an innovative bionic approach to improve emotion recognition in affective computing. Wu et al.¹⁶ analyzed 341 articles from the last 3 years following Preferred Reporting Items for Systematic

Reviews and Meta-analyses (PRISMA) requirements, summarized 16 publicly available datasets, and evaluated different neural network architectures. With increasing interest in graph neural networks and transformers, CNNs have become the most common. The review discussed technical features, research directions, and limitations of current methods, including patient variability, interpretable AI, dataset bias, and regional localization. Çokçetin and Uçar¹⁷ focused on different biometric modalities (e.g., electrocardiography [ECG], EEG, and photoplethysmography) and assessed their reliability and performance, as well as their evaluation between multimodal and unimodal systems. The analysis was planned according to PRISMA 2020 standards and filtered 80 articles from a total of 2,064 preliminary records retrieved from databases such as EBSCO and IEEE Xplore. The results showed that ECG systems had a high average accuracy (98.6%), whereas multimodal systems had a higher level of accuracy (more than 99%). Deep learning methods performed better than traditional methods, and dataset size and signature processing options had a significant effect on the results. The analysis demonstrated good performance of the biometric constructs, which need to be tested with larger samples, standardized norms, and further development of complementary biometric indicators to enhance their applicability. Wang et al.¹⁸ improved EEG signal evaluation by deriving 16 features across three domains: entropy, time-frequency, and second-order difference plot. Pearson correlation analysis, importance ranking, and Shapley additive explanations (SHAP) interpretability analysis were used to select the major discriminant functions, including spectral entropy (SE), spectral wavelet (SW), zero crossing rate (ZCR), short-time average (STA), central tendency measure (CTM) 2, and CTM 5. The ease of dimensional relaxation was facilitated by the relief regulations. The category accuracies achieved by grey wolf optimization with Cuckoo search (GWOCS) using the most desirable channel aggregate based on Fz, F7, Fp1, Fp2, F3, T3, P4, and C3 were 89.35% in move-validation and 81.12% in leave-one-subject-out (LOSO) validation. The study demonstrated the crucial roles of the prefrontal and temporal lobe structures in preventing dementia and concluded that the framework is efficient in rapid channel selection and in detecting the disorder. Xu et al.¹⁹ proposed control strategies in a perception–selection–execution hierarchy that specialize in four key activities: trajectory duplication, movement tracking, assistance on demand, and movement target

prediction. It describes the mechanisms, scenarios, and characteristics of several strategies, and even discovers challenges and limitations in power systems, manages coupling, and algorithm adaptation. Their study refined the end-effector control strategy to improve a general control framework for exoskeletons. Yu and Liu²⁰ proposed a method to enhance sentiment and emotion types using advanced preprocessing strategies, including noise elimination and tokenization, to obtain in-depth knowledge. Using an interest-based gated recurrent unit for sentiment classification can filter out important tasks, whereas the spatiotemporal optics algorithm can group sentiments by Twitter ID, location, and timestamp. The multi-beauty CatBoost algorithm then classifies these images into emotions, including anxiety and happiness, addressing overfitting and increasing accuracy. Implemented in Python 3, their model outperformed current methods, with an average accuracy of 92.04%, precision of 93.20%, recall of 92.58%, F-score of 91.8%, and computation time of 74.8 ms (**Table 1**).

3. Proposed work

We proposed a framework for EEG-based emotion recognition, integrating statistical feature preprocessing, advanced data augmentation, multi-architecture deep learning, and chaos-driven optimization (**Figure 1**). The primary objective of this framework is to ensure fair architectural comparison, stable model training, and robust classification performance across diverse neural network designs.

$$\mathcal{D} = \{(\mathbf{x}_i, y_i)\}_{i=1}^N \quad (1)$$

where \mathcal{D} denotes the EEG emotion dataset, $\mathbf{x}_i \in \mathbb{R}^d$ represents a d -dimensional statistical feature vector extracted from EEG signals, and $y_i \in \{1, 2, \dots, C\}$ denotes the corresponding emotion label, with C the emotion classes.

The objective is to learn a nonlinear mapping function:

$$f_\theta : \mathbb{R}^d \rightarrow \mathbb{R}^C \quad (2)$$

parameterized by θ , such that the predicted class probabilities:

$$\hat{\mathbf{y}}_i = \text{softmax}(f_\theta(\mathbf{x}_i)) \quad (3)$$

minimize classification error while maintaining strong generalization capability on unseen EEG samples^{17–20}.

Table 1. Summary of related studies in emotion recognition and EEG analysis.

Study	Data/Domain	Methodology	Performance
Guo et al. ⁸	EEG (DEAP)	ESN-TLC model integrating echo state networks (ESN), Transformer blocks, LSTM, and CNN	Accuracy: 93.9% (arousal), 94.2% (valence)
Zheng et al. ¹⁵	EEG (SEED, SEED-IV)	Gustatory-Emotion Coupling Model with Multiblock Attention Module (GECM-MBAM)	96.91% (SEED), 94.52% (SEED-IV)
Wu et al. ¹⁶	EEG (Systematic Review)	PRISMA-based review of 341 studies and 16 public datasets	-
Çokçetin and Uçar ¹⁷	EEG, ECG, PPG	PRISMA 2020 systematic review of unimodal vs multimodal biometrics	ECG: 98.6%; Multimodal: >99%
Wang et al. ¹⁸	EEG (dementia diagnosis)	Feature extraction (entropy, time-frequency, SODP) + Relief + GWOCS	89.35% (CV), 81.12% (LOSO)
Xu et al. ¹⁹	Exoskeleton control	Review of perception-decision-execution control strategies	-
Yu and Liu ²⁰	Social media text (Twitter)	SENTI-EMO: Attention-based GRU + STO + CatBoost	Accuracy: 92.04%, F1: 91.8%

Abbreviations: DEAP: Distributed Evolutionary Algorithms in Python; ECG: Electrocardiography; EEG: Electroencephalography; GRU: Gated recurrent unit; LSTM: Long short-term memory; PPG: Photoplethysmography; SENTI-EMO: Sentiment and emotion classification; SODP: Second-order difference plot; STO: Spatiotemporal optic.

3.1. Feature preprocessing and normalization

Given the raw statistical EEG features x_i , z -score normalization was applied to mitigate scale imbalance and improve numerical stability:

$$\tilde{x}_{ij} = \frac{x_{ij} - \mu_j}{\sigma_j} \quad (4)$$

where μ_j and σ_j denote the mean and standard deviation of the j -th feature computed from the training set, respectively. To address missing values, column-wise mean imputation is employed:

$$x_{ij} = \begin{cases} x_{ij}, & \text{if } x_{ij} \neq \text{NaN} \\ \frac{1}{N} \sum_{i=1}^N x_{ij}, & \text{otherwise} \end{cases} \quad (5)$$

3.2. Advanced data augmentation

To enhance robustness and reduce overfitting, multiple stochastic data augmentation techniques were applied during training^{21–23}.

3.2.1. Noise injection

Random noise is added to the input features:

$$\mathbf{x}' = \mathbf{x} + \epsilon \quad (6)$$

where ϵ is sampled from one of the following distributions:

$$\epsilon \sim \mathcal{N}(0, \alpha\sigma), \epsilon \sim \text{Laplace}(0, \alpha\sigma), \epsilon \sim \mathcal{U}(-\alpha, \alpha)$$

3.2.2. Random feature scaling

Noise injection is employed as a stochastic data augmentation strategy to enhance model robustness and improve generalization when learning from EEG-derived statistical features.^{24–28} EEG signals are inherently noisy due to physiological artifacts (e.g., eye blinks and muscle activity), sensor displacement, and environmental interference (**Figure 2**). Rather than treating noise solely as an undesirable factor, controlled noise injection enables the model to learn invariant and discriminative representations that are resilient to real-world perturbations. Feature-wise scaling is applied as:

$$\mathbf{x}' = \mathbf{x} \odot \mathbf{s}, s_j \sim \mathcal{U}(0.8, 1.2) \quad (7)$$

3.2.3. Time warping

Time warping is an augmentation technique designed to simulate temporal variability in EEG-derived features by introducing controlled nonlinear distortions along the temporal axis.^{29–32} EEG signals are inherently time-dependent, and emotional responses often manifest with varying onset times, durations, and temporal dynamics across subjects and trials (**Figure 3**). Time warping enables the learning model to become invariant to such temporal misalignments while preserving the underlying emotional patterns. For time-dependent features, interpolation-based temporal

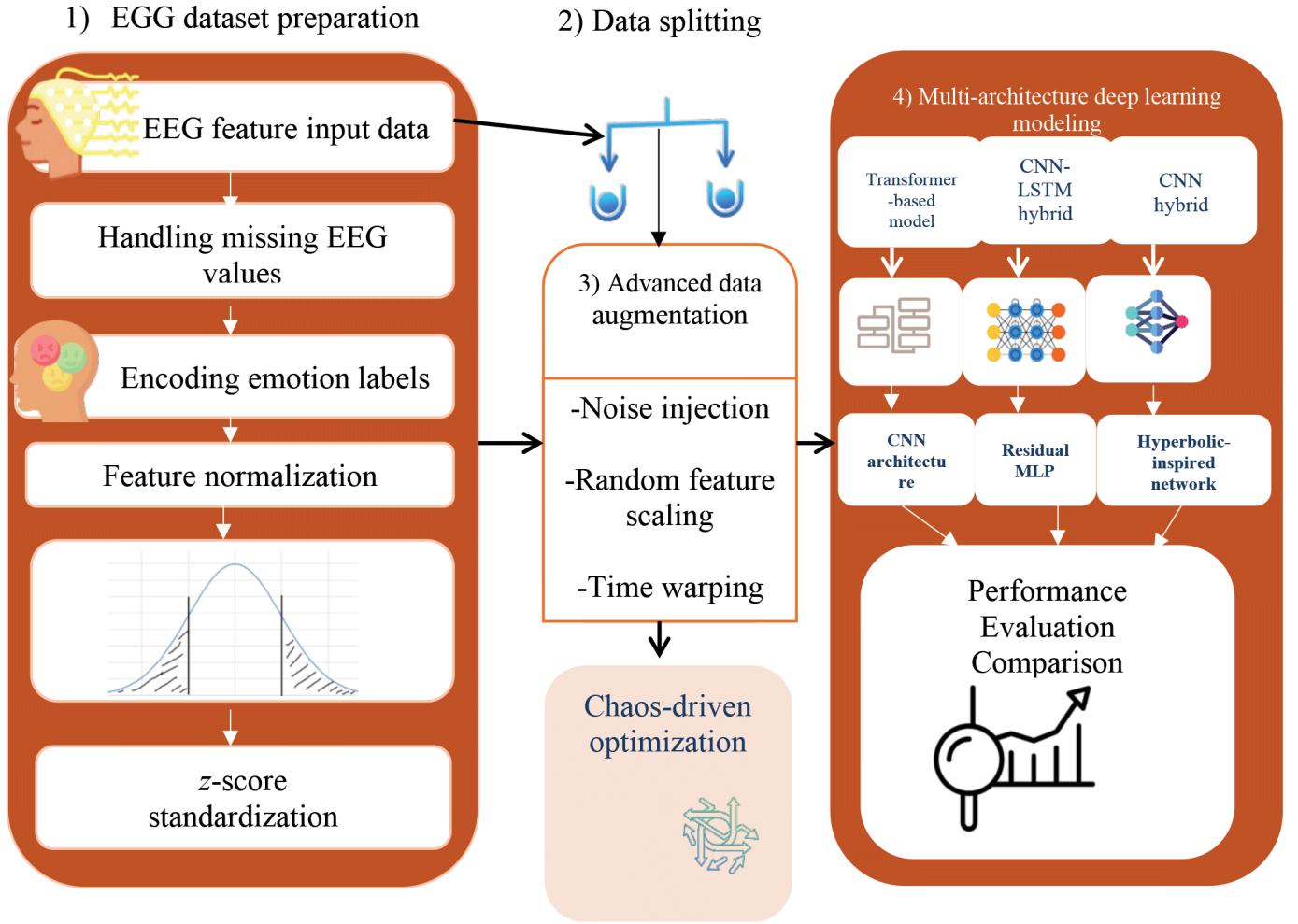


Figure 1. Overall framework of the proposed electroencephalography (EEG)-based emotion recognition system

warping is applied:

$$\mathbf{x}'(t) = \text{Interp}(\mathbf{x}(\phi(t))) \quad (8)$$

where $\phi(t)$ represents a nonlinear temporal distortion function.

3.2.4. Feature masking

Feature masking is a regularization-based data augmentation technique that enhances model robustness by randomly suppressing a subset of input features during training.^{33–35} In EEG-based emotion recognition, extracted statistical features may contain redundancy, noise, or channel-specific bias.^{36–38} Feature masking encourages the learning model to avoid over-reliance on any single feature or frequency component and instead learn distributed, robust representations. Random feature-level dropout is applied to simulate signal degradation:

$$x'_j = \begin{cases} x_j, & \text{with probability } p \\ 0, & \text{otherwise} \end{cases} \quad (9)$$

3.3. Deep learning architectures

Five neural architectures were implemented to model EEG emotion patterns under a unified experimental setup.

3.3.1. Transformer-based architecture

Transformer-based architecture was designed to model global dependencies among high-dimensional EEG statistical features by leveraging self-attention mechanisms (**Figure 4**).

Unlike convolutional or recurrent models that focus on local or sequential relationships, the Transformer enables direct interactions between all feature dimensions, making it well-suited for capturing the complex inter-feature correlations inherent in EEG signals. Input features are linearly projected into a latent space:

$$\mathbf{z} = \mathbf{W}_p \mathbf{x} + \mathbf{b}_p \quad (10)$$

Self-attention is computed as:

$$\text{Attention}(\mathbf{Q}, \mathbf{K}, \mathbf{V}) = \text{softmax}\left(\frac{\mathbf{Q}\mathbf{K}^\top}{\sqrt{d_k}}\right) \mathbf{V} \quad (11)$$

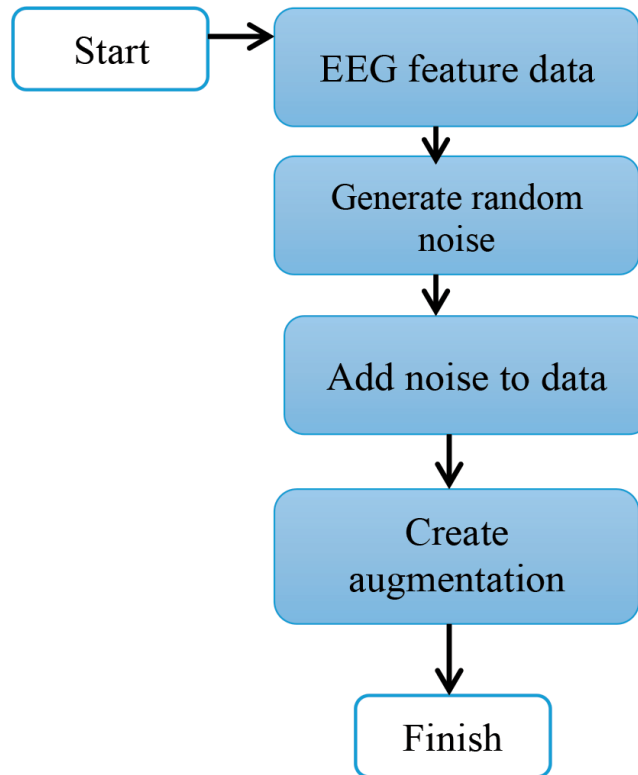


Figure 2. Flowchart illustrating the noise-based data augmentation process applied to electroencephalography (EEG) feature data

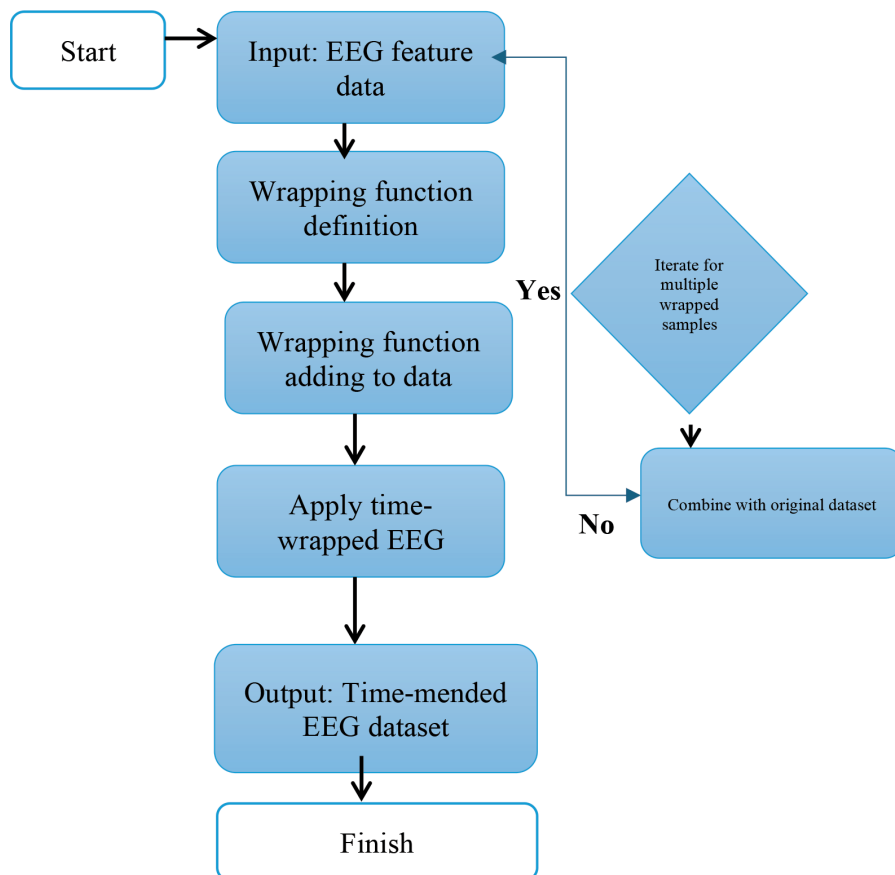


Figure 3. Flowchart of the time-warping augmentation process applied to electroencephalography (EEG) feature data

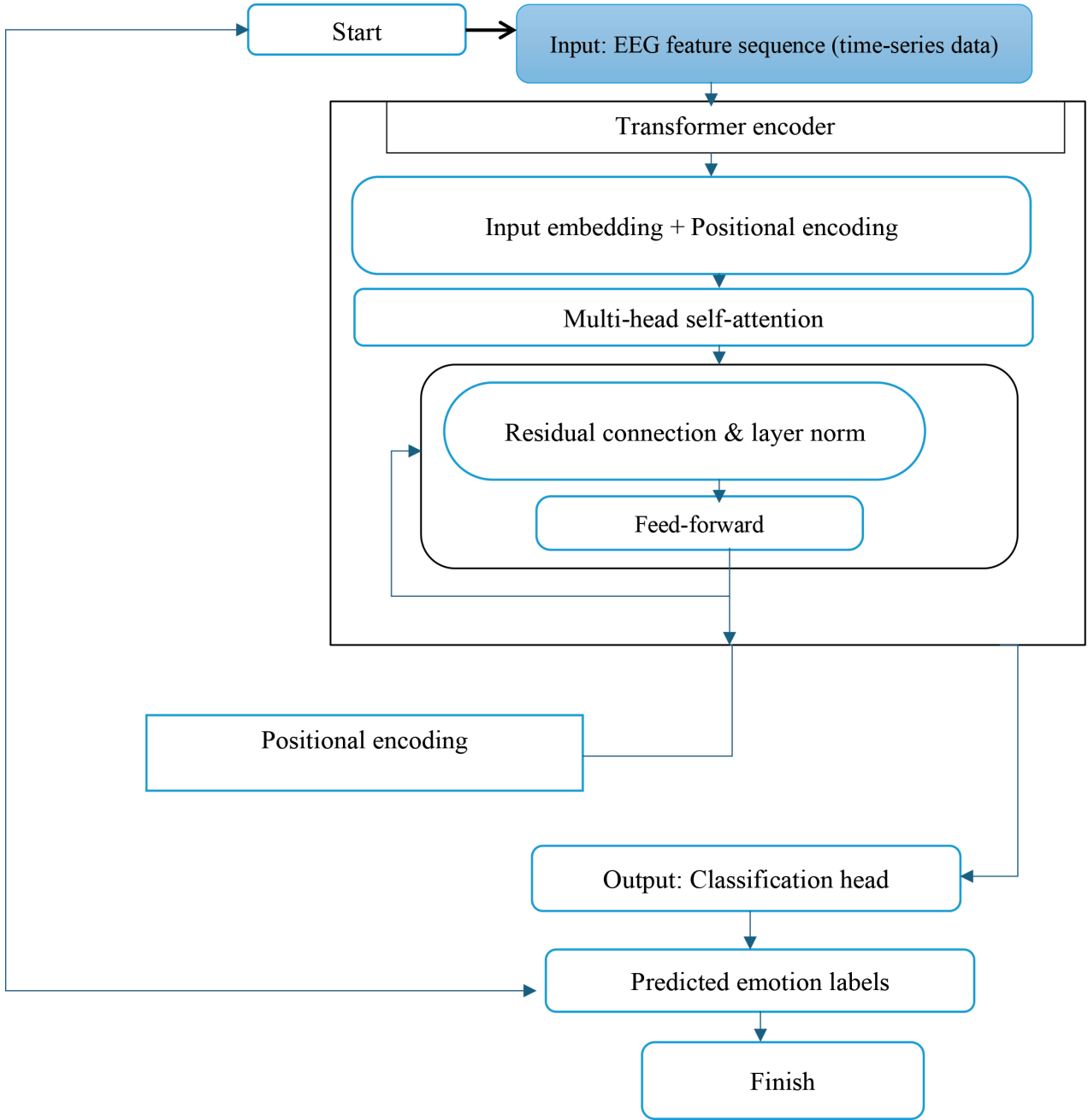


Figure 4. Transformer-based architecture for electroencephalography (EEG) time-series emotion classification

Transformer layers capture long-range dependencies before classification.

3.3.2. CNN–LSTM hybrid architecture

The CNN–LSTM hybrid architecture was designed to jointly capture spatial feature correlations and temporal dependencies within high-dimensional EEG-derived statistical features (**Figure 5**). CNNs are effective at learning local spatial patterns, while LSTM networks excel at modeling temporal dynamics.^{39,40} Their integration provides a powerful framework for EEG-based emotion recognition, where both interactions and sequential dependencies are critical. Local spatial feature extraction is performed

using 1D convolution:

$$h_c = \text{Conv1D}(x) \quad (12)$$

Temporal dependencies are modeled via LSTM:

$$h_t = \text{LSTM}(h_c) \quad (13)$$

3.3.3. Residual multilayer perceptron

The residual MLP architecture was designed to address the challenges of training deep fully connected networks on high-dimensional EEG statistical features (**Figure 6**). Standard MLP often suffers from vanishing gradients and performance degradation as network depth increases. To overcome these limitations, residual connections are incorporated to facilitate efficient gradient flow

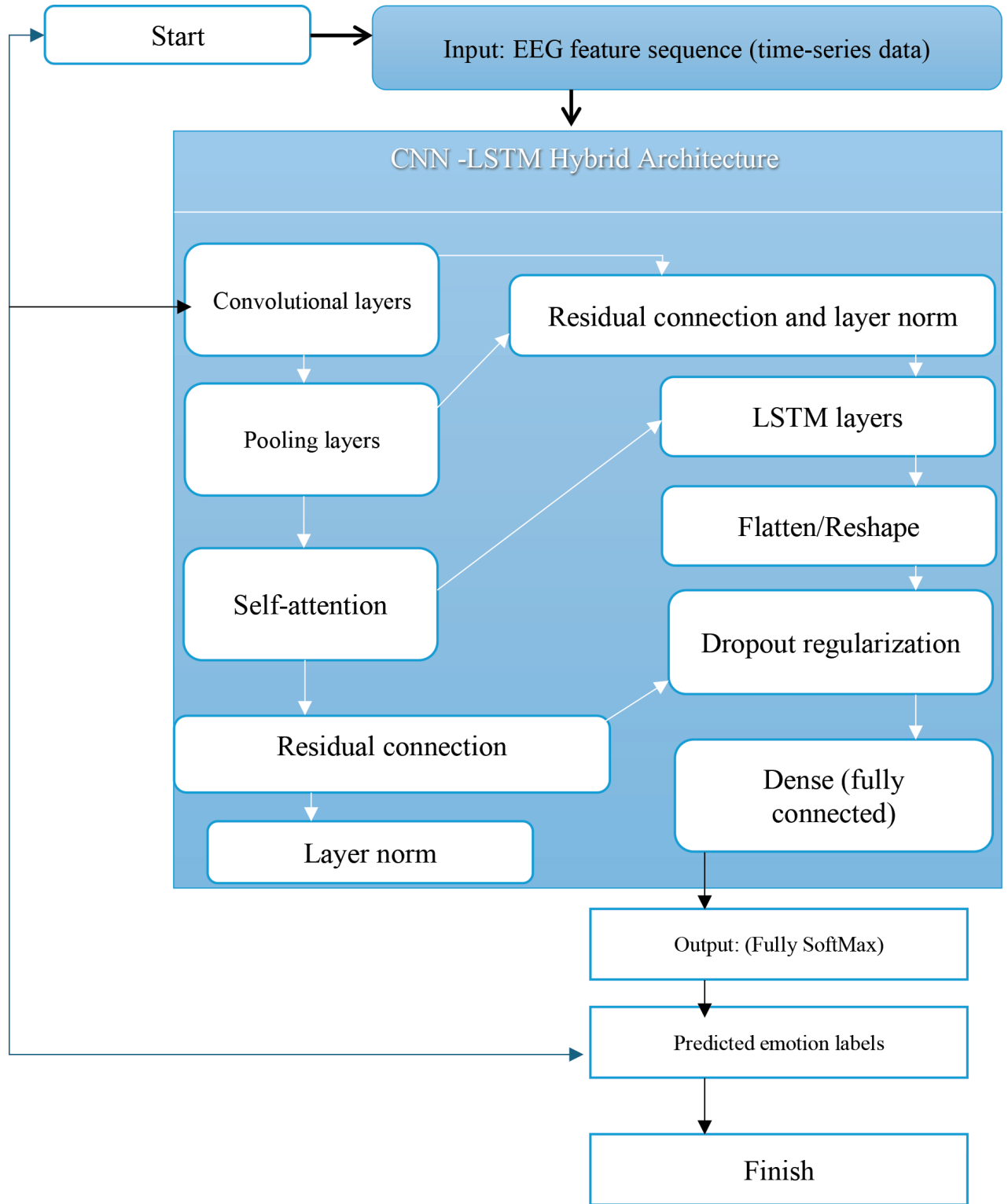


Figure 5. Convolutional neural network–long short-term memory (CNN–LSTM) hybrid architecture with self-attention for electroencephalography (EEG) time-series emotion classification

and stabilize optimization. Residual connections stabilize deep learning:

$$h_{l+1} = F(h_l) + h_l \quad (14)$$

where $F(\cdot)$ denotes a nonlinear transformation block.

3.3.4. Capsule network

Capsule networks were designed to preserve hierarchical relationships and spatial dependencies between features by grouping neurons into vector-valued entities called capsules. Unlike traditional neural networks that encode information using scalar activations, capsules represent fea-

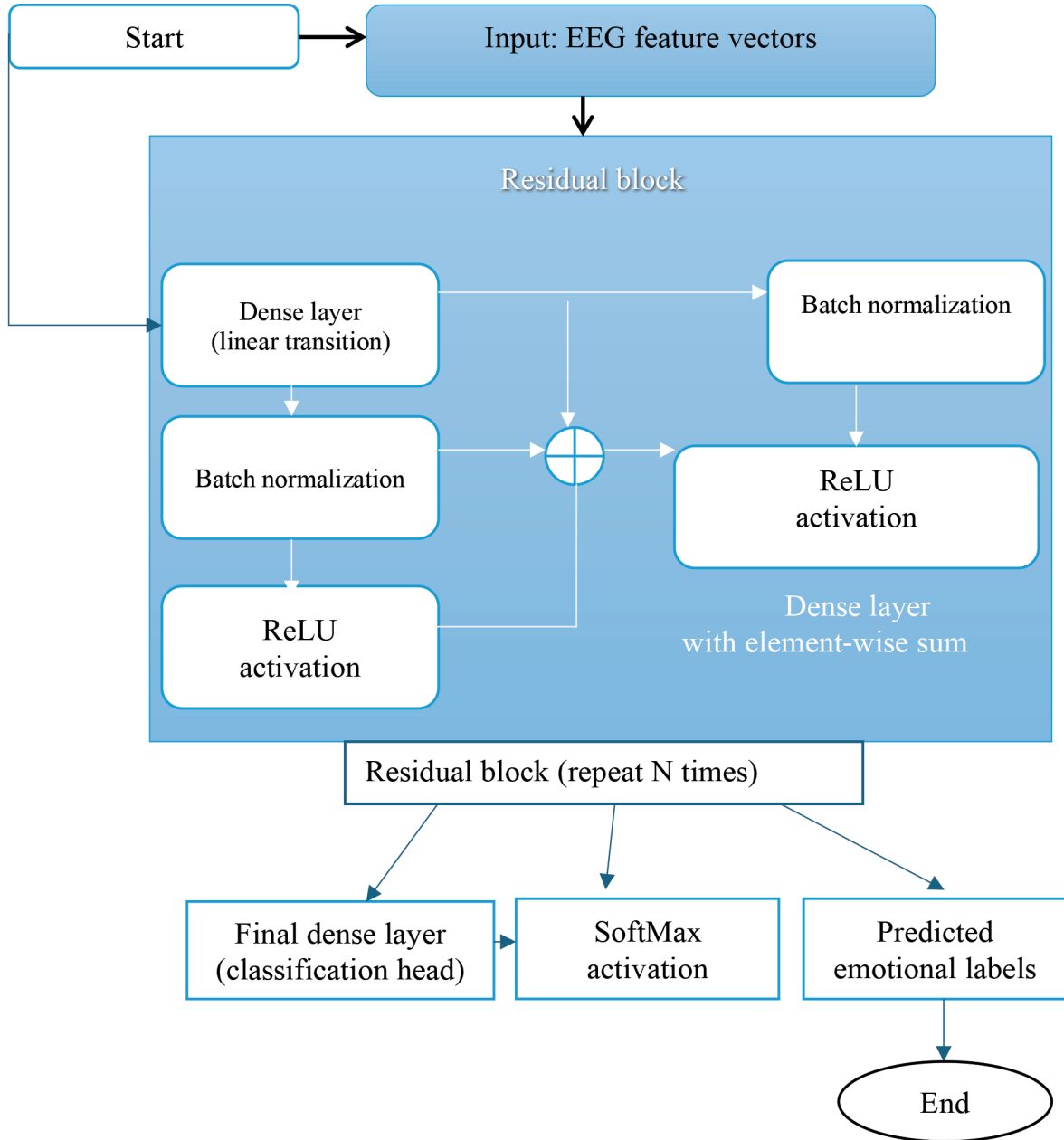


Figure 6. Residual multilayer perceptron (MLP) architecture for electroencephalography (EEG) feature-based emotion classification

tures as vectors whose length encodes the presence probability of a pattern, while their orientation captures instantiation parameters (**Figure 7**). This property is particularly advantageous for EEG emotion recognition, where emotional states arise from coordinated interactions across multiple EEG features and channels. Primary capsules are formed as:

$$u_i = W_i x \quad (15)$$

Capsule outputs are concatenated and classified, preserving part-whole relationships in EEG representations.

3.3.5. Hyperbolic-inspired network

The hyperbolic-inspired network was designed to enhance nonlinear representation learning by exploiting the properties of hyperbolic tangent activations. EEG emotion patterns are highly nonlinear, nonstationary, and distributed across multiple statistical features (**Figure 8**). Hyperbolic functions provide smooth saturation behavior and symmetric activation ranges, making them well-suited for modeling such complex brain dynamics while maintaining numerical stability. Hyperbolic tangent activation enhances nonlinear representation:

$$h_{l+1} = \tanh(W_l h_l + b_l) \quad (16)$$

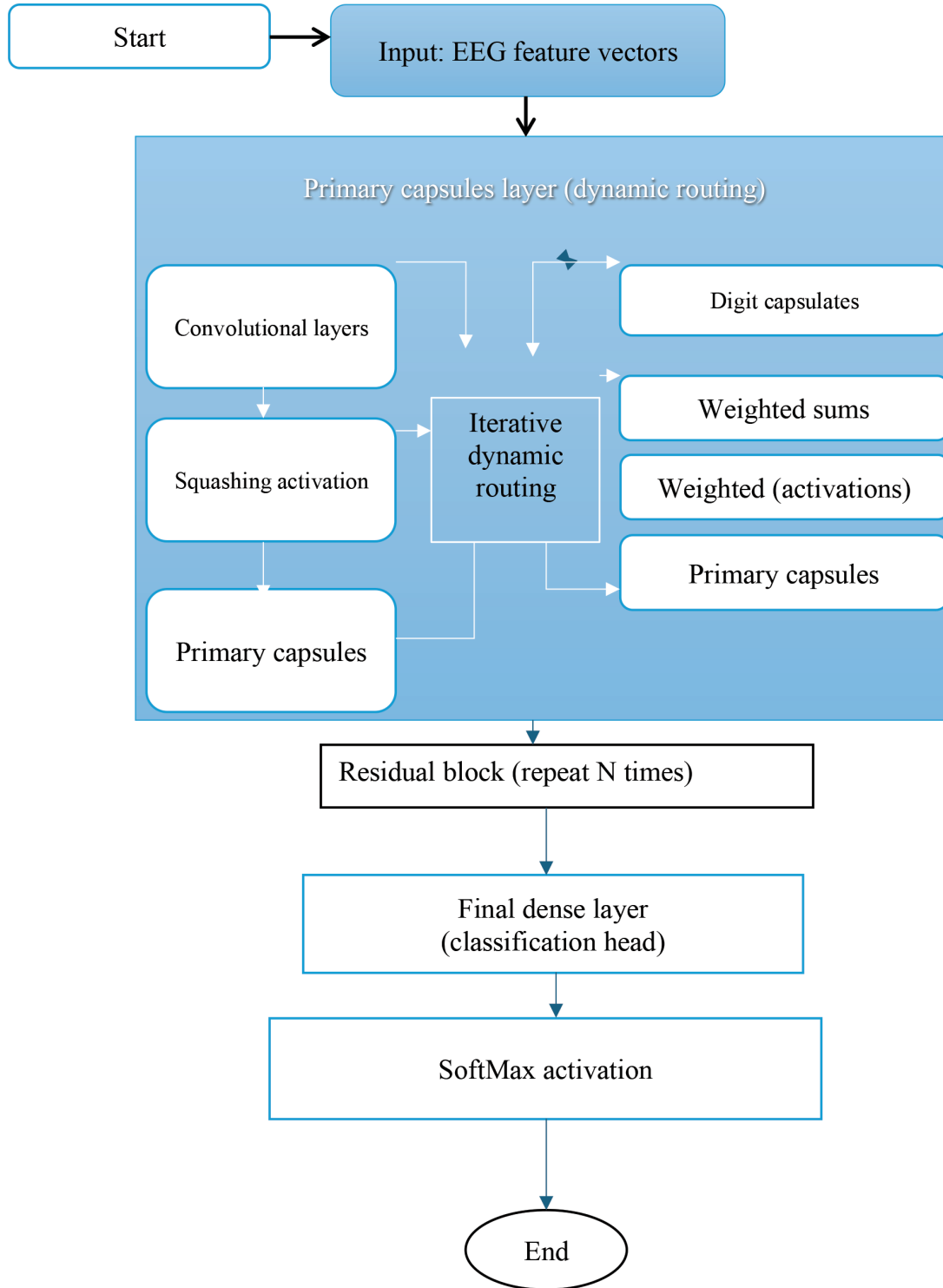


Figure 7. Capsule network architecture with dynamic routing for electroencephalography (EEG) feature-based emotion classification

3.4. Chaotic optimization strategy

Deep neural networks trained on high-dimensional EEG feature spaces often suffer from slow convergence, premature stagnation, and entrapment in local minima, particularly when the dataset is limited or the class distributions are imbalanced (**Figure 9**). To address these challenges, a chaos-driven optimization strategy is incorporated into the training process to dynamically regulate the

learning rate and enhance exploration during parameter updates. To enhance training stability and escape local minima, a chaos-driven learning rate mechanism was introduced. The chaotic sequence was generated as:

$$x_{t+1} = ax_t(1 - x_t), a = 3.8 \quad (17)$$

To ensure stable training, gradient clipping is applied during backpropagation to prevent ex-

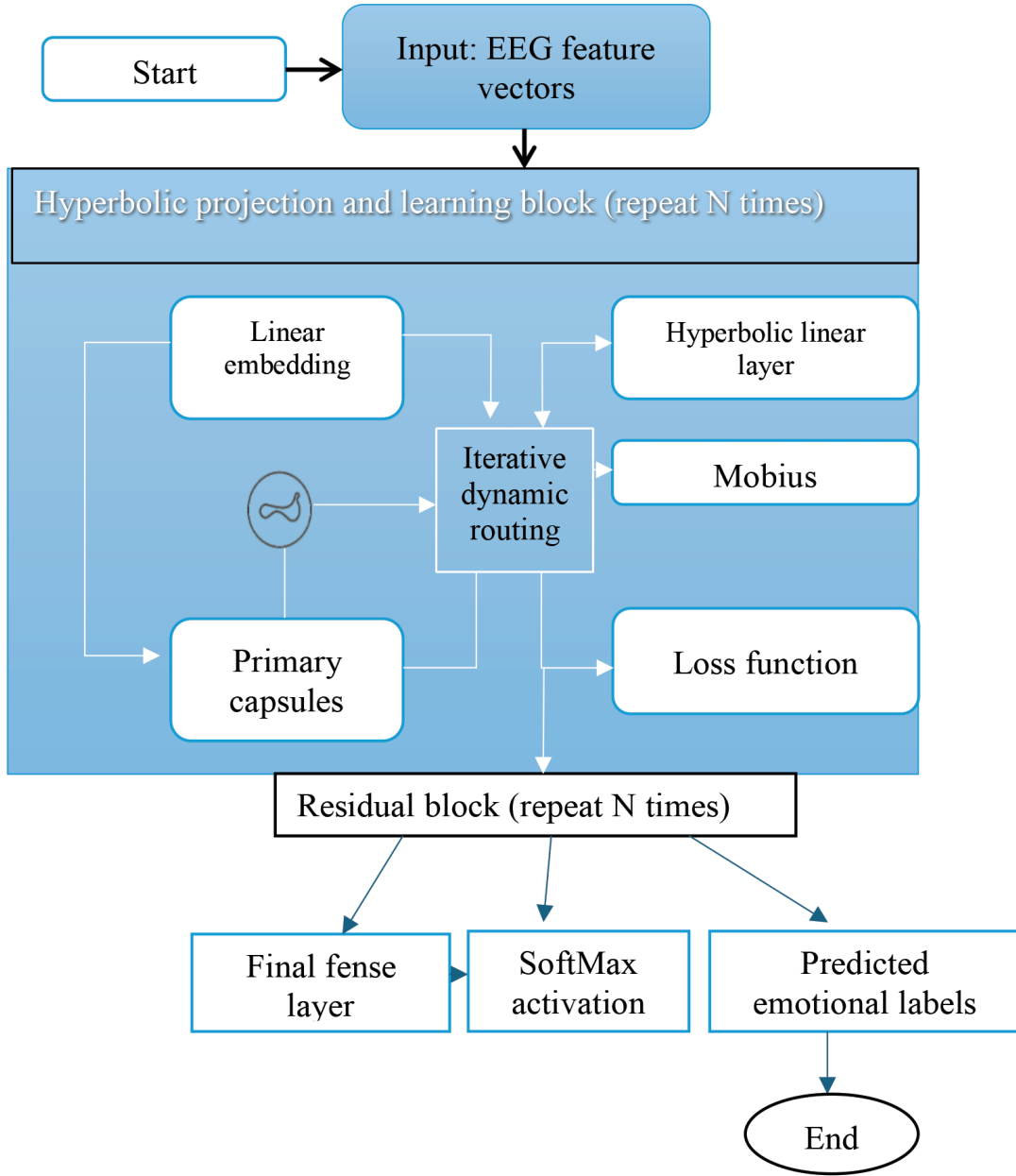


Figure 8. Hyperbolic-inspired neural architecture for electroencephalography (EEG) feature-based emotion classification

ploding gradients. Specifically, norm-based clipping is used to constrain the magnitude of gradients before updating the model parameters. This is particularly important in the proposed framework, where chaotic learning rate modulation, random noise augmentation, and the incorporation of a hyperbolic linear layer may increase gradient variability. By limiting gradient magnitudes, the model achieves more stable convergence and improved robustness.

Furthermore, the chaotic optimization strategy is applied globally to the entire training process rather than being restricted to a specific architectural component. The chaotic sequence dynamically modulates the learning rate, thereby influencing all network parameters during opti-

mization. Although the hyperbolic linear layer benefits from this strategy due to its nonlinear representation capability, it is not the sole component affected by the chaotic mechanism.

The learning rate at iteration t is defined as:

$$\eta_t = \eta_0(0.5 + x_t) \quad (18)$$

where η_0 is the base learning rate. This dynamic adjustment introduces controlled stochasticity into the optimization process.

A class-weighted cross-entropy loss is employed:

$$\mathcal{L} = - \sum_{c=1}^C w_c y_c \log(\hat{y}_c) \quad (19)$$

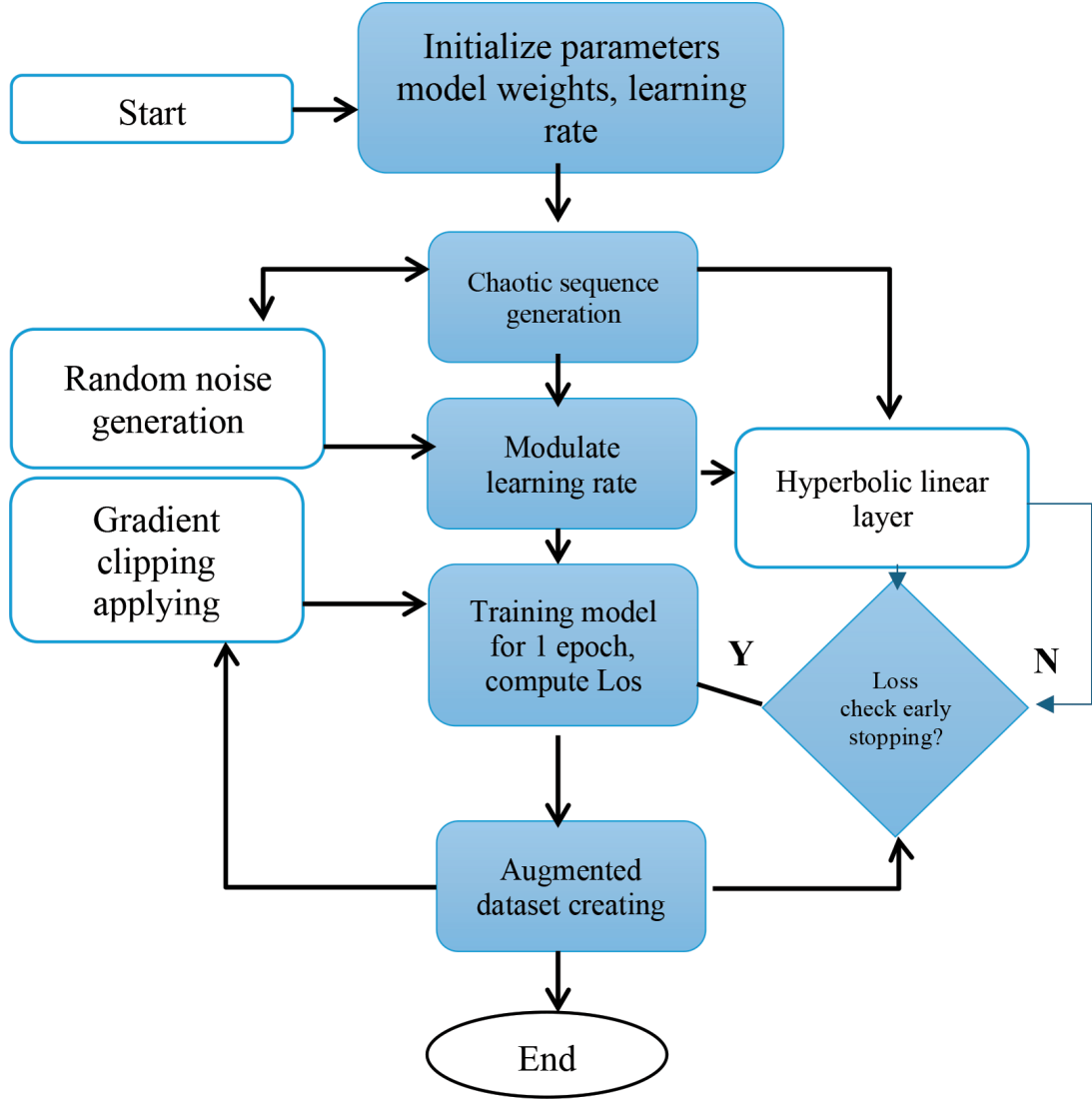


Figure 9. Chaotic optimization strategy for adaptive training of the proposed electroencephalography (EEG) classification model

where w_c compensates for class imbalance. Optimization is performed using AdamW:

$$\theta_{t+1} = \theta_t - \eta_t \frac{\hat{m}_t}{\sqrt{\hat{v}_t + \epsilon}} \quad (20)$$

4. Results

4.1. Dataset description

The data consisted of EEG brainwave records, with features extracted using an original statistical strategy. The dataset was designed to facilitate research in the fields of affective computing, mental state recognition, and brain-machine interfaces. The EEG data were recorded using a controlled, yet realistic, experimental model (Table 2). Two healthy subjects (one male and one female) were recruited to record data with the Muse EEG headband (InteraXon, Canada), a non-invasive consumer-grade device with dry electrodes. The frontal and temporal brain regions

of interest in emotion processing were recorded using four EEG channels (TP9, AF7, AF8, and TP10), placed according to the international 10–20 system. Positive, neutral, and negative were three emotional states provoked using carefully selected audiovisual stimuli. Every state of emotion was documented for three minutes, along with a six-minute baseline recording in the neutral resting condition. Ecological validity was increased with naturalistic video stimuli and a real-world recording setting, whereas inter-subject variability and signal drift were reduced with the help of a baseline session (Table 3). Emotional elicitation was produced through well-known film and multimedia content used in the framework of affective computing studies. Emotions of loss and grief caused negative feelings, whereas musical sequences, nature pictures, and humor generated positive feelings. The variety of stimulus sources and types of scenes provided strong emotional

Table 2. Electroencephalography (EEG) data collection protocol

Parameter	Description
Participants	2 healthy subjects (1 male, 1 female)
Emotional states	Positive, neutral, negative
Recording duration per state	3 min
Baseline recording	6 min (resting neutral state)
EEG device	Muse EEG headband
Electrode type	Dry electrodes
EEG channels	TP9, AF7, AF8, TP10
Electrode placement standard	International 10–20 system
Data acquisition environment	Non-invasive, real-world setting

Table 3. Emotional stimuli used for data collection

Emotion	Stimulus	Source/Publisher	Scene description
Negative	<i>Marley and Me</i>	Twentieth Century Fox	Death scene
Negative	<i>Up</i>	Walt Disney Pictures	Opening death scene
Negative	<i>My Girl</i>	Imagine Entertainment	Funeral scene
Positive	<i>La La Land</i>	Summit Entertainment	Opening musical sequence
Positive	<i>Slow Life</i>	BioQuest Studios	Nature timelapse footage
Positive	<i>Funny Dogs</i>	MashupZone	Humorous dog video compilation

involvement and minimized bias associated with stimuli, thereby enhancing the applicability of the learned representations in general.

4.2. Feature extraction and signal processing

Raw EEG signals were initially temporally resampled to guarantee that all recordings had similar signal alignment. EEG signals were not analyzed using handcrafted frequency-domain features; instead, they were mathematically modeled in the time domain, and statistical descriptors of the dynamics of brainwaves were obtained. This approach retains the temporal nature and can be compared with machine learning and deep learning. The feature vectors were constructed to provide a common input space across all considered models, enabling a fair comparison of the various network architectures. **Table 4** identifies the feature extraction and processing pipeline.

The dataset’s class distribution is shown in **Table 5**, with an almost equal distribution across the three emotional groups. The neutral, negative, and wonderful lessons include 716, 708, and 708 samples, respectively, for a total of 2,132. This balanced distribution reduces class bias and minimizes the need for aggressive reweighting during training. The dataset was divided into training and validation sets using an 80:20 split (**Table 6**),

ensuring sufficient data for both learning and generalization evaluation. As presented in **Table 7**, each EEG sample is represented by 2,547 statistical features, resulting in a high-dimensional input space.

The classification task consisted of three emotion classes. Class weights were computed to further compensate for minor class imbalance, ensuring stable optimization and balanced decision boundaries during training. The proposed HybridRobertaEEG architecture, detailed in **Table 8**, employs a deep feature processing pipeline composed of fully connected layers with progressive dimensionality reduction. Gaussian error linear unit activation functions, batch normalization, and dropout regularization were applied to improve convergence stability and prevent overfitting. A multi-head interest mechanism operating in a 128-dimensional latent space was incorporated to improve feature interaction modeling. The very last fusion and class layers map discovered representations of the three-emotion training.

Model complexity statistics are reported in **Table 9**, indicating a total of 1.61 million trainable parameters. Training was conducted on a GPU enabled by compute unified device architecture, using a chaotic optimization strategy based on a logistic map to dynamically modulate learning be-

Table 4. Feature extraction and processing strategy

Step	Description
Signal preprocessing	Temporal resampling of raw electroencephalography (EEG) signals
Feature extraction	Original statistical feature extraction strategy
Temporal modeling	EEG waves mathematically represented in time domain
Output features	Statistical descriptors of brainwave dynamics
Intended use	Machine learning and deep learning models

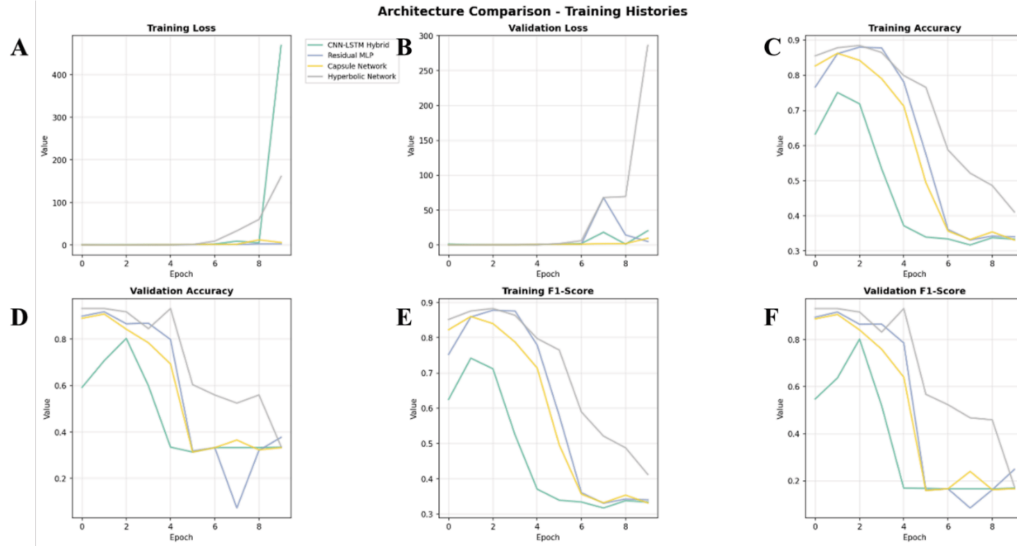


Figure 10. Comparison of training and validation performance across different deep learning architectures. (A) Training loss. (B) Validation Loss. (C) Training accuracy. (D) Validation accuracy. (E) Training F1-score. (F) Validation F1-score

Abbreviations: CNN: Convolutional neural network; LSTM: Long short-term memory; MLP: Multilayer perceptron.

Table 5. Class distribution of the dataset

Class	Number of samples
Neutral	716
Negative	708
Positive	708
Total	2,132

havior. The model converged quickly and achieved significant performance improvements within the first three epochs. The validation accuracy rose to 90.16% in Epoch 1 and 91.80% in Epoch 3, and the validation loss steadily decreased, indicating effective generalization. **Table 10** reports training performance across epochs. **Table 11** shows the best validation performance, with an accuracy of 91.80% at Epoch 3 and a corresponding approximate learning rate of 8.26×10^{-4} . Even though training was set to 50 epochs, early convergence indicates the usefulness of the chaotic optimization strategy for speeding up learning and preventing overfitting.

Table 12 shows a thorough comparison of various chaotic-optimized deep learning architectures. The CNN-LSTM hybrid model performed poorly, with a maximum validation rate of 70.73, which could be attributed to its limited capacity to model high-dimensional statistical features. Conversely, the residual MLP and the capsule network achieved high validation accuracies of 91.80% and 90.87%, respectively. The hyperbolic network was the most appropriate, achieving the highest overall performance with a validation accuracy of 93.21% and the lowest validation loss (0.197). These findings emphasize the benefits of hyperbolic representations for hierarchical and complex emotional patterns in EEG data, especially when incorporated with chaotic optimization strategies (**Figure 10** and **11**).

5. Conclusion

In this paper, we present a unified and systematic framework for EEG-based emotion recognition that integrates statistical feature extrac-

Table 6. Training and validation data split

Dataset Split	Number of Samples	Percentage (%)
Training	1,705	80
Validation	427	20
Total	2,132	100

Table 7. Feature and class configuration

Parameter	Value
Feature type	Electroencephalography statistical features
Number of features	2,547
Number of classes	3
Class weights	[0.3347, 0.3306, 0.3347]

Table 8. HybridRobertaEEG model architecture summary

Component	Description
Electroencephalography feature processor	Fully connected layers (2,547 \rightarrow 512 \rightarrow 256 \rightarrow 128)
Activation function	Gaussian error linear unit
Normalization	Batch normalization
Regularization	Dropout ($p = 0.3$)
Attention mechanism	Multi-head attention (128 dimensions)
Fusion layer	Dense layers (128 \rightarrow 256 \rightarrow 128 \rightarrow 64 \rightarrow 3)
Output classes	3 (neutral, negative, positive)

Table 9. Model complexity

Metric	Value
Total parameters	1,612,163
Trainable parameters	1,612,163
Optimization device	Compute unified device architecture (GPU)
Optimization strategy	Chaotic optimization (logistic map)

Table 10. Training performance across epochs

Epoch	Train loss	Train accuracy (%)	Validation loss	Validation accuracy (%)
1	0.8689	68.50	0.5076	90.16
2	0.6197	84.05	0.4755	90.63
3	0.5660	86.22	0.4464	91.80

tion with chaos-enhanced deep learning optimization. By evaluating five representative neural architectures—Transformer-based, CNN–LSTM hybrid, residual MLP, capsule network, and hyperbolic-inspired network—under identical ex-

perimental conditions, the work provides a fair and comprehensive comparison of architectural effectiveness for affective EEG classification. The experimental results demonstrate that chaos-driven optimization, implemented through a

Table 11. Best validation performance

Metric	Value
Best validation accuracy	91.80%
Epoch achieved	3
Learning rate (approx.)	8.26×10^{-4}
Number of epochs	50 (early best at Epoch 3)

Table 12. Performance comparison of chaotic-optimized deep learning architectures

Architecture	Parameters	Best validation accuracy (%)	Best validation loss	Training time (s)
CNN–LSTM hybrid	43,971	70.73	0.581	21.21
Residual MLP	754,319	91.80	0.226	21.78
Capsule network	168,323	90.87	0.237	19.43
Hyperbolic network	688,975	93.21	0.197	19.09

Abbreviations: CNN: Convolutional neural network; LSTM: Long short-term memory; MLP: Multilayer perceptron.

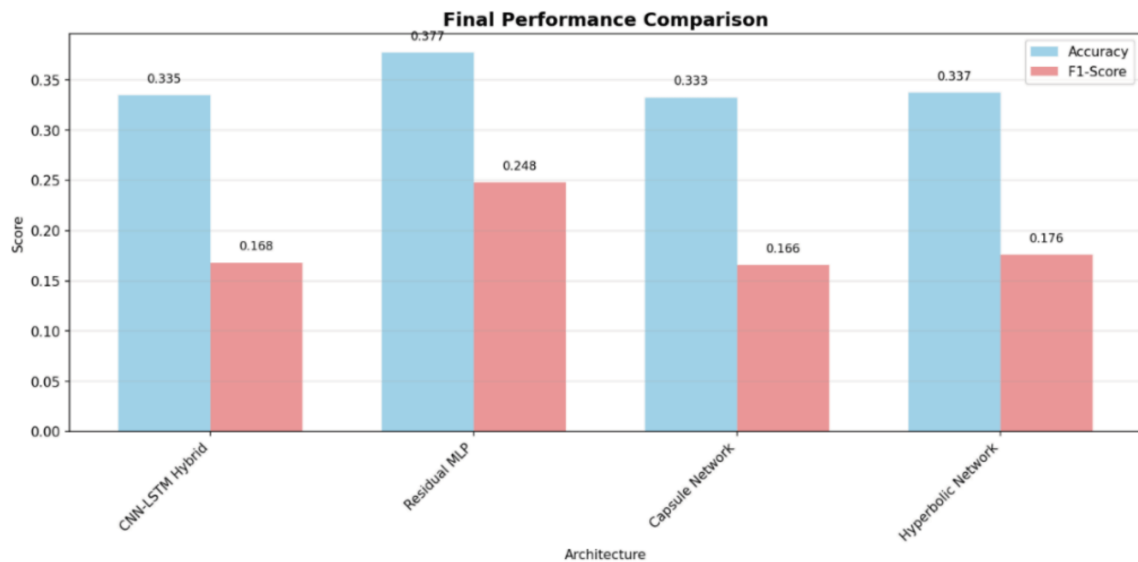


Figure 11. Final performance comparison of the evaluated deep learning architectures in terms of accuracy and F1-score

Abbreviations: CNN: Convolutional neural network; LSTM: Long short-term memory; MLP: Multilayer perceptron.

logistic-map-based learning rate modulation, significantly improves training stability, accelerates convergence, and enhances generalization performance across all evaluated models. Among the tested architectures, the hyperbolic-inspired network achieved the best overall performance, reaching a validation accuracy of 93.21% with the lowest validation loss and reduced training time. The residual MLP and capsule network also exhibited strong performance, confirming the effectiveness of residual learning and dynamic routing mechanisms for modeling EEG features. In contrast, the CNN–LSTM hybrid model showed compar-

atively lower accuracy, highlighting the limitations of sequential architectures when applied to high-dimensional statistical EEG features. Despite the promising results, this study has several limitations that warrant further investigation. The dataset was collected from a limited number of participants, which may restrict the generalizability of the models across diverse populations and emotional expressions. Future work should incorporate larger, multi-subject datasets with greater demographic diversity to improve robustness and cross-subject generalization. Incorporating frequency-domain, time–frequency,

and graph-based EEG representations could further enhance emotional discrimination.

Acknowledgments

None.

Funding

The authors extend their appreciation to Prince Sattam bin Abdulaziz University for funding this research work through the project number (PSAU/2025/01/36818).

Conflict of interest

The authors declare that they have no known competing financial interests or personal relationships that could have appeared to influence the work reported in this paper.

Author contributions

Conceptualization: All authors

Formal analysis: All authors

Methodology: All authors

Writing—original draft: All authors

Writing—review & editing: All authors

Availability of data

The data are available from the corresponding author upon reasonable request.

AI tools statement

All authors confirm that AI tools were used only for grammatical and stylistic issues.

References

1. Li C, Zhang Z, Song R, Cheng J, Liu Y, Chen X. EEG-based emotion recognition via neural architecture search. *IEEE Trans Affect Comput.* 2021;14(2):957-968. <https://www.doi.org/10.1109/TAFFC.2021.3130387>
2. Hasan R, Islam SMR. A comparative analysis of emotion recognition from EEG signals using temporal features and hyperparameter-tuned machine learning techniques. *MethodsX.* 2025;103468. <https://www.doi.org/10.1016/j.mex.2025.103468>
3. Keelawat P, Thammasan N, Numao M, Kijirikul B. A comparative study of window size and channel arrangement on EEG-emotion recognition using deep CNN. *Sensors (Basel).* 2021;21(5):1678. <https://www.doi.org/10.3390/s21051678>
4. Joloudari JH, Maftoun M, Nakisa B, Alizadehsani R, Yadollahzadeh-Tabari M. Complex emotion recognition system using basic emotions via facial expression, EEG, and ECG signals: a review. Preprint. *arXiv.* 2024. <https://www.doi.org/10.48550/arXiv.2409.07493>
5. Kumari N, Anwar S, Bhattacharjee V. A comparative analysis of machine and deep learning techniques for EEG evoked emotion classification. *Wirel Pers Commun.* 2023;128(4):2869-2890. <https://www.doi.org/10.1007/s11277-022-10076-7>
6. Haider M. Cooperative chameleon search optimization enabled deep ensemble classifier for emotion recognition using EEG signal. *Comput Methods Biomech Biomed Eng.* 2025;1-23. <https://www.doi.org/10.1080/10255842.2025.2568979>
7. Yildirim E, Kaya Y, Kiliç F. A channel selection method for emotion recognition from EEG based on swarm-intelligence algorithms. *IEEE Access.* 2021;9:109889-109902. <https://www.doi.org/10.1109/ACCESS.2021.3100638>
8. Guo X, Liang R, Xu S, Dong L, Liu Y. An investigation of echo state network for EEG-based emotion recognition with deep neural networks. *Biomed Signal Process Control.* 2026;111:108342. <https://www.doi.org/10.1016/j.bspc.2025.108342>
9. Jehosheba Margaret M, Masoodhu Banu NM. Performance analysis of EEG-based emotion recognition using deep learning models. *Brain Comput Interfaces.* 2023;10(2-4):79-98. <https://www.doi.org/10.1080/2326263X.2023.2206292>
10. Muniyandi AP, Padmanandam K, Subbaraj K, et al. An intelligent emotion prediction system using improved sand cat optimization technique based on EEG signals. *Sci Rep.* 2025;15(1):8782. <https://www.doi.org/10.1038/s41598-025-89904-2>
11. Huang H, Deng Y, Hao B, Liu W, Tu X, Zeng G. Emotion recognition method using U-Net neural network with multichannel EEG features and differential entropy characteristics. *IEEE Access.* 2024. <https://www.doi.org/10.1109/ACCESS.2024.3497160>
12. Mir WA, Anjum M, Shahab S. Deep-EEG: an optimized and robust framework and method for EEG-based diagnosis of epileptic seizure. *Diagnostics (Basel).* 2023;13(4):773. <https://www.doi.org/10.3390/diagnostics13040773>
13. Zhang S, Ling C, Wu J, et al. EEG-ERnet: emotion recognition based on rhythmic EEG convolutional neural network model. *J Integr Neurosci.* 2025;24(8):41547. <https://www.doi.org/10.31083/JIN41547>
14. Maria MA, Akhand MAH, Hossain AA, Kamal MAS, Yamada K. A comparative study on prominent connectivity features for emotion recognition from EEG. *IEEE Access.* 2023;11:37809-37831.


- <https://www.doi.org/10.1038/s41598-023-40786-2>
15. Zheng W, Peng Y, Zhang A, Yuan Q. EEG-based emotion identification from nerve conduction mechanisms: a gustatory-emotion coupling model combined with multiblock attention module. *Expert Syst Appl.* 2026;298:129855. <https://www.doi.org/10.1016/j.eswa.2025.129855>
16. Wu Y, Lu, L, Xu A, et al. Neural networks for epilepsy detection and prediction with EEG signals: a systematic review. *Artif Intell Rev.* 2025;59(1):30. <https://www.doi.org/10.1007/s10462-025-11441-1>
17. Çokçetin B, Uçar MK. A PRISMA-based systematic review on advances in identity recognition and authentication using human biometric signals (2018–2023). *Biomed Eng Online.* 2026. <https://www.doi.org/10.1186/s12938-025-01508-z>
18. Wang R, Xu H, Ma Y, Che Y. Research on the classification of EEG signals for dementia and its interpretability using the GWOCS algorithm. *Cogn Neurodyn.* 2025;20(1):1. <https://www.doi.org/10.1007/s11571-025-10348-5>
19. Xu X, Chen C, Sun Z, et al. Research on control strategy of lower limb exoskeleton robots: a review. *Sensors (Basel).* 2026;26(2):255. <https://www.doi.org/10.3390/s26020355>
20. Yu F, Liu JM. A deep learning-based framework for sentiment and emotion classification of social media messages during pandemic periods. *J Circuits Syst Comput.* 2025;35(3):2550413. <https://www.doi.org/10.1142/S0218126625504134>
21. Eisa MM, Alnaggar MH. Hybrid rough-genetic classification model for IoT heart disease monitoring system. In: Magdi DA, Helmy YK, Mamdouh M, Joshi A, eds. *Digital Transformation Technology. Lecture Notes in Networks and Systems*, vol 224. Springer. 2022:437-451. https://www.doi.org/10.1007/978-981-16-2275-5_27
22. Abdella MH, Hawash AA, Zahran OE, et al. Smart tour guide: a novel artificial intelligence system for replacing human guides in cultural heritage sites. *Egypt J Artif Intell.* 2024;3(1). <https://www.doi.org/10.21608/ejai.2024.226751.1017>
23. Hassan E, Bhatnagar R, Shams MY. Advancing scientific research in computer science by ChatGPT and LLaMA—A review. In: Sai PHVST, Potnuru S, Avcar M, Kar VR, eds. *Intelligent Manufacturing and Energy Sustainability.* Springer; 2023:23-37. https://www.doi.org/10.1007/978-981-99-6774-2_3
24. Karthiga M, Suganya E, Sountharajan S, et al. EEG-based smart emotion recognition using meta heuristic optimization and hybrid deep learning techniques. *Sci Rep.* 2024;14(1):30251. <https://www.doi.org/10.1038/s41598-024-80448-5>
25. Ibrahim MA, Ali ME, Ahmed MN, et al. A low-cost approach for drowning detection and alertness. *Egypt J Artif Intell.* 2024;3(1). <https://www.doi.org/10.21608/ejai.2024.223796.1012>
26. Davarzani S, Masihi S, Panahi M, et al. A comparative study on machine learning methods for EEG-based human emotion recognition. *Electronics (Basel).* 2025;14(14):2744. <https://www.doi.org/10.3390/electronics14142744>
27. Hassan E, El-Rashidy N, Elbedwehy S, et al. Exploring the frontiers of image super-resolution: a review of modern techniques and emerging applications. *Neural Comput Appl.* 2025;37(22):17913-17961. <https://www.doi.org/10.1007/s00521-025-11331-1>
28. Hamzah HA, Abdalla KK. EEG-based emotion recognition systems: comprehensive study. *Helvion.* 2024;10(10). <https://www.doi.org/10.1016/j.helivon.2024.e31485>
29. Kargarnovin S, Hernandez C, Farahani FV, Karwowski W. Evidence of chaos in electroencephalogram signatures of human performance: a systematic review. *Brain Sci.* 2023;13(5):813. <https://www.doi.org/10.3390/brainsci13050813>
30. Hassan E, Bhatnagar R, Abd El-Hafeez T, Shams MY. Detection of suicide and depression for early intervention and initiative-taking mental health-care. In: *Proc IEEE ISPPCC.* 2025:99-104. <https://www.doi.org/10.1109/ISPPCC66872.2025.11039547>
31. Alnaggar MH, El-Dosuky M, Rashad M. A novel multimodal biometric template security based on nano-scale reaction-diffusion morphogenesis. *J Comput Theor Nanosci.* 2018;15(6-7):1979-1982. <https://www.doi.org/10.1166/jctn.2018.7522>
32. Chhabra H, Vempati R, Chauhan U, et al. Automated human emotion recognition from EEG signals using chaotic local binary pattern and ensemble learning. *Int J Mach Learn Cybern.* 2026;17(1):12. <https://www.doi.org/10.1007/s13042-025-02822-7>
33. Hasoun RK. Hybrid optimized feature selection and deep learning method for emotion recognition that uses EEG data. *Iraqi J Comput Inform.* 2025;51(1):1-18. <https://www.doi.org/10.25195/ijci.v51i1.545>
34. Shams MY, Hassan E, Gamil S, et al. Skin disease classification: a comparison of ResNet50, MobileNet, and Efficient-B0. *J Curr Multidiscip Res.* 2025;1(1):1-7.

- <https://www.doi.org/10.21608/jcmr.2025.327880.1002>
35. Flower TML, Singh SCE, Jaya T, Devadhas GG. EEG-based emotion recognition: a systematic review of traditional and deep learning methods. *Science*. 2025;15:100180.
<https://www.doi.org/10.70389/PJS.100180>
 36. Tan S, Tang Z, He Q, et al. Automatic detection and prediction of epileptic EEG signals based on nonlinear dynamics and deep learning: a review. *Front Neurosci*. 2025;19:1630664.
<https://www.doi.org/10.3389/fnins.2025.1630664>
 37. Kumar BA, Suresh HN, Ranjitha S. EEG-based assessment of suicidality risk: an integrated framework with self-adaptive chaotic cuckoo search and AttentionBiSqueezeNet. *Eng Technol Appl Sci Res*. 2026;16(1):32391-32397.
<https://www.doi.org/10.48084/etasr.14247>
 38. Saber A, Hassan E, Elbedwehy S, Awad WA, Emara TZ. Leveraging ensemble convolutional neural networks and metaheuristic strategies for advanced kidney disease screening and classification. *Sci Rep*. 2025;15(1):12487.
<https://www.doi.org/10.1038/s41598-025-93950-1>
 39. Al-Qammaz AYA. *An enhanced computational model based on social spider optimization algorithm for EEG-based emotion recognition*. Dissertation. Universiti Utara Malaysia; 2019.
<https://www.doi.org/10.14419/ijet.v7i2.15.11373>
 40. Hassan E, Saber A, Alqahtani O, El-Rashidy N, Elbedwehy S. An innovative approach to


advanced voice classification of sacred Quranic recitations through multimodal fusion. *Egypt Inform J*. 2025;30:100640.

<https://www.doi.org/10.1016/j.eij.2025.100640>

Zahraa Tarek received the Ph.D. in computer science from Mansoura University, Egypt. She is currently a professor in information technology with the Faculty of Computers and Artificial Intelligence, Mansoura University, Egypt. She has published many research articles in prestigious international conferences and reputable journals. She is also a reviewer for many journals. Her ongoing work continues to support both academic innovation and practical technological advancements across the AI and Big Data landscape.

 <https://orcid.org/0000-0001-9389-2850>

Esraa Hassan was born in Kafrelsheikh, Kafrelsheikh, Egypt, in 1992. She received a B.Sc. Degree in Computer Science and an M.Sc. Degree in Computer Science from Mansoura University, Egypt, in 2013 and 2018, respectively. She received her Ph.D. in computer science from Mansoura University, Egypt, in 2022. She is currently a lecturer at the Faculty of Artificial Intelligence, Kafrelsheikh University, Egypt. She has published many research articles in prestigious international conferences and reputable journals. She is also a reviewer for many journals. Her research interests include machine learning, deep learning, optimization, and bioinformatics.

 <https://orcid.org/0000-0002-1021-717>

An International Journal of Optimization and Control: Theories & Applications (<https://accscience.com/journal/ijocta>)



This work is licensed under a Creative Commons Attribution 4.0 International License. The authors retain ownership of the copyright for their article, but they allow anyone to download, reuse, reprint, modify, distribute, and/or copy articles in IJOCTA, so long as the original authors and source are credited. To see the complete license contents, please visit <http://creativecommons.org/licenses/by/4.0/>.